Original Article
Inhibition of retinal angiogenesis by ω-3 PUFAs via modulating TLR4/NF-κB signal pathway in microglia

Zhi Li*, Qin Li*, Genguo Wang, Yi Huang, Xiaochun Mao, Yanfang Zhang, Xueyan Wang

*Department of Ophthalmology, Xiangyang Central Hospital, Affiliated Hospital of Hubei University of Arts and Science, Hubei, China. *Equal contributors.*

Abstract: Omega-3 polyunsaturated fatty acids (ω-3 PUFAs) can inhibit retinal angiogenesis by anti-inflammation. PPAR-γ suppresses inflammation through impeding TLR4/NF-κB signal pathway. This study aims to determine the effect of ω-3 PUFAs on retinal angiogenesis and explore the possible mechanisms by using oxygen-induced retinopathy (OIR) mouse model. The retinal angiogenesis and microglia number were counted by using fluorescent microscopy and expressions of PPAR-γ, TLR4, p-IκBα, p-p65, TNF-α and IL-1β were determined by qRT-PCR and western blotting. *In vitro* cultured microglia was stimulated by LPS and treated with ω-3 PUFAs for comparing gene expression of PPAR-γ, TLR4, p-IκBα, p-p65, TNF-α and IL-1β. Tube formation assay measured the effect of ω-3 PU-FAs. Our result showed that retinal angiogenesis and microglia were apparently enhanced in OIR model mice. ω-3 PUFAs intervention up-regulated PPAR-γ expression, and suppressed expressions of TLR4, p-IκBα, p-p65, TNF-α and IL-1β, and played an inhibitory role in angiogenesis or microglia activation. ω-3 PUFAs also weakened effect of LPS, suppressed TLR4/NF-κB signal pathway activity, inflammatory factor release or tube formation. In conclusion, ω-3 PUFAs inhibits microglia activation or reginal angiogenesis via enhancing PPAR-γ expression and restricting TLR4/NF-κB signal pathway.

Keywords: ω-3 PUFAs, TLR4/NF-κB, retinal angiogenesis, microglia cells

Introduction

Retinal neovascular disease (RND), as a type of severe blinding disease, consists of retinopathy of prematurity (ROP), diabetic retinopathy (DR) and age-related macular degeneration (AMD) [1]. Although certain therapeutic efficacy has been obtained by anti-VEGF drugs [2], it can also give rise to side-effect due to the unfavorable interference on normal development of retinal vessels [3].

Omega-3 polyunsaturated fatty acids (ω-3 PUFAs) represents necessary fatty acid in human body. Current studies showed that the inhibition of retinal angiogenesis was not related with VEGF expression inhibition, but was associated with certain roles of ω-3 PUFAs in anti-inflammatory response [4, 5]. ω-3 PUFAs can exert anti-inflammatory effects via modulating lipid metabolism, altering membrane fluidity and signal transduction, changing adhe-

sion molecule expression, and suppressing synthesis or release of inflammatory mediators [6]. Moreover, recent evidence showed that activation or change of peroxisome proliferator-activated receptor gamma (PPAR-γ) was also implicated with ω-3 PUFAs [6-8]. Microglia (MG) is a tissue specific monocyte-macrophage cell lineage in central nervous system (CNS) and retina, and plays important roles in immune modulation, angiogenesis and traumatic repair [9]. Previous finding indicated that higher number and activation of MG plays were critical for retinal angiogenesis during RNDs such as oxygen-induced retinopathy (OIR) and DR [10, 11]. Various studies demonstrated that activation of PPAR-γ could suppress expression of inflammatory factors via inhibiting TLR4/NF-κB signal pathway activation [12, 13]. Therefore, we speculated that ω-3 PUFAs could suppress retinal angiogenesis via changing PPAR-γ expression and inhibiting TLR4/NF-κB signal pathway activation, which further decreased the synthe-

sis, expression and release of pro-vascular inflammatory factors from MG. Our pilot study revealed that by enhancing retinal ω-3 PUFAs expression, retinal angiogenesis can be suppressed by up-regulating PPAR-γ expression [14]. Therefore, this study generated a mouse OIR model, on which ω-3 PUFAs were injected via tail veins, in order to identify the effect of ω-3 PUFAs on retinal angiogenesis.

Materials and methods

Major reagent and materials

DMEM/F12 culture medium, FBS, penicillin-streptomycin and trypsin were purchased from Gibco (US). RNA extraction kit Rneasy MiNi Kit, fluorescent quantitative PCR kit TransScript Green One-Step qRT-PCR SuperMix were from TransGen Biotech (China). Rabbit anti-PPAR-γ, TLR4, β-actin antibody were purchased from Abcam (US). Rabbit anti-p-IκBα, p-p65 and p65 antibody were obtained from CST (US). HRP conjugated secondary antibody was purchased from Bio-Rad (US). FITC-dextran was collected from Kaixin Bio (China). ω-3 PUFAs were purchased from Huarui Pharm (China). Endothelial cell line HUVEC was provided by Baili Biotech (China). Endothelial cell medium (ECM) was purchased from ScienCell (US). Matrigel was offered by BD bioscience (US). PE-Iba1 flow cytometry antibody was bought from Biolegend (US).

OIR mouse model generation

Healthy SPF grade C57BL/6J mice (7 days old) and gestation female mice were purchased from Silaike Laboratory Animal (China), and were housed in self-made closed oxygenated chambers, each of which contained 2 gestation females. The oxygen flow of chamber was kept between 1.2 and 1.5 L/min, and the outflow tube was connected to model CY-12C oxygenated meter. Oxygen concentration inside the chamber was monitored 6~8 times daily for keeping at 75±2%, whilst environmental temperature was kept at 23±2°C. General conditions of juvenile and gestation mice were observed. Gestation mice were alternatively placed under normal conditions for 6~8 h observation, and were put back into the closed oxygenated chamber. After 5-day feeding in high-oxygenated chamber, mice were further kept for 5 days under normal oxygen concentra-

tion. Mice under normal conditions were used as the control group. This study was approved by experimental animal ethical committee, and all animal experimental protocols followed ARVO guidance.

ω-3 PUFAs treatment on OIR mice

OIR model mice received 100 g/L ω-3 PUFAs (1 mL/kg) by injection into tail veins since D0. Equal volume of ω-3 PUFAs was injected on each morning during 10 consecutive days. OIR model mice receiving equal volume of saline were used as the control.

Retinal fluorescein angiography

After anesthesia, FITC-dextran solution was perfused into the heart. Mouse eyeballs were removed and fixed in 4% paraformaldehyde for 3 h in dark. Cornea, lens and vitreous were removed by cutting the edge. Retina was separated from outer sclera and choroid from corneoscleral limbus. Retina was carefully removed and laid on the slide. Using optical disc as the center, retina was cut from four quadrants. Blocking reagent containing anti-bleaching buffer was added, followed by observation under fluorescent microscope. Image-Pro Plus 6.0 was used to measure the relative area of vessel-free and angiogenesis areas among the whole retina.

HE staining for retinal slices

Mice were sacrificed by cervical dislocation. Eyeballs were removed and were fixed in Boun's solution for 4 h, followed by 70% ethanol fixation. Gradient ethanol was added for dehydration. Tissues were embedded in paraffin and prepared for 4 μm consecutive sagittal slices. Five slices were selected from each eyeball with 30 μm distances. Those slices showing optic nerve cross-sections were removed. HE staining was performed by dewax in xylene for 10 min (2 times), followed by rehydration in gradient ethanol, and 15 min hematoxylin staining for 15 min. By three times of rinsing in tap water, sliced were treated in HCl-ethanol for 30 s, and were rinsed under tap water for 3 times. 1% ammonia was added, followed by rinsing in tap water. 1% eosin was added for 3 min staining, followed by gradient ethanol dehydration, xylene treatment, resin mounting and observation under light filed microscope.

Counting of retinal angiogenesis

Retina was removed and immersed in PBS solution containing 1% Triton X-100 and 1% BSA, and was cultured at 4°C for 12 h blocking. Retina was immersed in 1:100 Lectin solution with FITC labels at 4°C, in dark incubation for 12 h to label retinal vascular endothelial cells. The slice was rinsed in PBS for three times. Retinal was cut from 4 radial axis, and was paved with inner face laying upwards. By treating with 50% glycerol, number of retinal vascular angiogenesis was counted under microscopy.

MG cell count in retina by immunofluorescence

Mice were sacrificed and eyeballs were removed. After fixation in 4% paraformaldehyde for 120 min, cornea and lens were removed. By dehydration in gradient sucrose, tissues were embedded in OCT for preparing frozen slices at the thickness of 8 μm, which were dried in room temperature and rinsed in PBS for three times. By blocking in PBS containing 1% Triton X-100 and 1% BSA, slices were cultured in Iba1 primary antibody (1:200) at 4°C overnight, followed by three times of PBS rinsing. Alexa flour 594 labelled secondary antibody (1:400) was added for room temperature incubation. By DAPI staining for nucleus, coverslips were mounted for observation under a fluorescent microscope. The number of positive cells in 5 mm length was counted.

Flow cytometry identification for retinal MG cells

Mice were sacrificed and eyeballs were removed. Retinal vessels were carefully under microscope. Retina was separated and digested in 0.125% trypsin at 37°C for 20 min, followed by PBS rinsing, 80% methanol fixation and 0.1% PBS-Tween permeabilization. The retina was blocked in PBS containing 10% goat serum for 20 min, and was cultured in PE labelled Iba1 antibody for 30 min at 4°C. By two times of PBS washing, Iba1 positive MG cells were measured by Gallios flow cytometry.

Separation and culture of retinal MG

Under sterile conditions, mouse eyeballs were collected and removed from retinal vessels under stereoscopes. Retina was separated and digested in 0.125% trypsin for 20 min at 37°C. Undigested tissue debris was filtered out, whilst filtrate was centrifuged at 300 g for 5 min. Cells were re-suspended in DMEM/F12 complete medium with 10% FBS, and were seeded into poly-lysine coated 6-well plate with incubation in a 37°C chamber with 5% CO_2. Culture medium was changed every 4 days. After 2-week culture, culture plated was vibrated at 100 g for 60 min. The supernatant was centrifuged at 300 g for 10 min. Cells were re-suspended in DMEM/F12 medium containing 10% FBS and were seeded in coating-free 6-well plate for incubation in a 37°C chamber with 5% CO_2. Culture medium was changed every other day. Cells were passed when reaching 80% confluence. Cells at log-growth phase were used for further experiments.

LPS activation and ω-3 PUFAs of retinal MG cells

Retinal MG cells were seeded into 6-well plate at $3×10^5$ per well density. After 24 h attached growth, cells were assigned into four groups: control group with normal culture; LPS activation group with adding 200 ng/mL LPS, ω-3 PUFAs treatment group receiving 100 μg/mL ω-3 PUFAs, and LPS+ω-3 PUFAs treatment group. All cells were cultured for 48 h for collecting and further assays.

Tube formation assay and MG cell co-culture

HUVEC cells were kept in ECM and in a chamber with 5% CO_2 at 37°C. When cells were at log-growth phase, cells were digested with trypsin for tube formation assay. Matrigel was added into 24-well plate (200 μL per well) for 37°C incubation for 30 min. HUVEC cells after trypsin digestion were re-suspended in ECM, and were added into 24-well plate with Matrigel on the bottom. Each well received about $2×10^5$ cells. Low chamber of 24-well plate was inoculated with HUVEC cells in tube formation assay. Transwell chamber was inserted into 24-well plate. The upper chamber of Transwell was seeded with $2×10^5$ retinal MG cells. When being activated by 200 ng/mL LPS, MG cells also received 0 or 100 μg/mL ω-3 PUFAs treatment. After 48 h co-culture, cells were collected for further assays, along with tube formation.
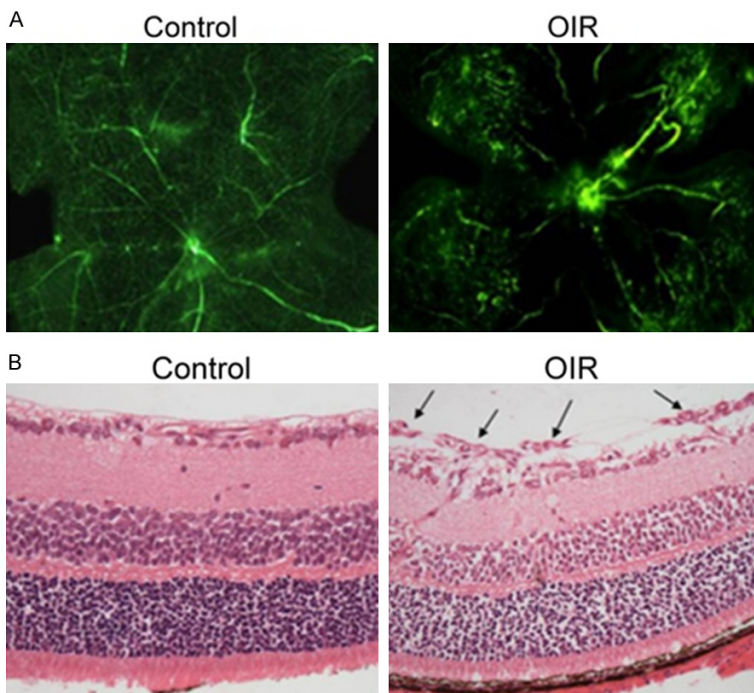
Figure 1. Successful generation of OIR mouse model. A. Fluorescein angiography of retina showed irregular vascular morphology, unevenly vascular cavity, decrease of angiogenesis in certain areas; B. HE staining indicated that vascular endothelial nucleus in OIR model group was increased.

Table 1. Serum-free area, *de novo* angiogenesis area and vessel number

	Control group	OIR group
Vessel-free area ratio (%)	0	16.27±1.31*
De novo angiogenesis area (%)	0	1.96±0.16*
Vessel number	93.3±1.2	156.5±2.3*

Note: *, P<0.05 comparing between OIR and control group.

qRT-PCR for gene expression

TransScript Green One-Step qRT-PCR SuperMix was used for one-step qRT-PCR to test relative gene expression level. In a 20 μL system, 1 μg template RNA, 0.2 μM forward primer, 0.2 μM reverse primer, 10 μL 2XTransStart Tip Green qPCR SuperMix, 0.4 μL One-Step RT Enzyme Mix, 0.4 μL Passive Reference Dye II and RNase-free water were mixed. qRT-PCR conditions were: 45°C 5 min, and 94°C 30 s, followed by 40 cycles each containing 94°C 5 s, and 60°C 30 s. Gene expression was measured on ABI 7500 real time fluorescent quantitative PCR cycler.

Western blot for protein expression

Protein samples were mixed with loading buffer, and separated by SDS-PAGE using 10%

separating gel and 5% condensing gel. Proteins were then transferred to nitrocellulose membrane, which was blocked by 5% defatted milk powder in PBS. Primary antibody (PPAR-γ at 1:400, TLR4 at 1:400, p-IκBα at 1:100, IκBα at 1:200, p-p65 at 1:100, p65 at 1:200 and β-actin at 1:600) was added for overnight incubation. The membrane was then washed in PBST for three times, and was incubated with streptavidin-HRP conjugated secondary antibody (1:5000 dilution) for 1 h under room temperature. By rinsing in PBST for three times, enhanced illuminance was used for development and testing for protein expression.

Statistical analysis

SPSs 18.0 was used for data analysis. Measurement data were presented as mean ± standard deviation (SD), and were compared by t-test or Mann-Whitney U test. A statistical significance was defined when P<0.05.

Results

Successful generation of OIR mouse model

Observation on retinal vascular fluorescein angiography showed complete vascularization of retina in normal group, and equal distribution of vascular without vessel-free region were also found (**Figure 1A**). In OIR model mice, irregular vascular morphology, unevenly vascular cavity diameter, striking decrease of angiogenesis in certain areas were shown. At the boundary between vessel-free region and normal vessels, *de novo* retinal vascular buffed (**Figure 1A**). HE staining also showed dramtically higher vascular endothelial nucleus in OIR model group, compared to those in normal oxygenated mice (**Figure 1B**). Significantly higher ratios of serum-free area, *de novo* vascular area ratio and vessel number were presented in OIR model mice compared to that of normal control group (P<0.05) (**Table 1**).
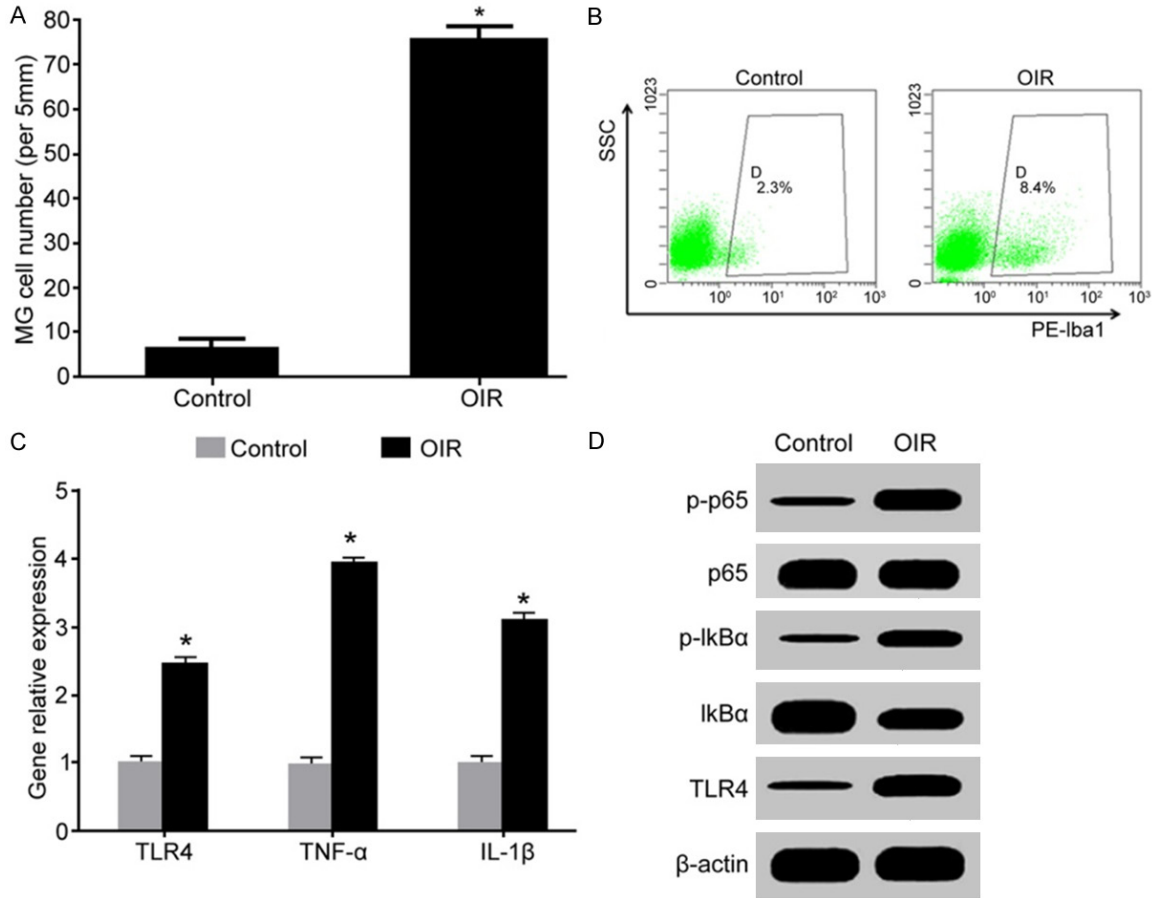
Figure 2. MG activation, enhanced TLR4 expression and NF-κB activity in OIR mouse retina. A. MG cell count in retina of OIR group was significantly magnified compared to control group; B. Flow cytometry showed Iba1 positive rate in OIR group was obviously increased; C. qRT-PCR for mRNA expressions indicated that TLR4, TNF-α, IL-1β were significantly elevated in OIR group compared to control group; D. Western blot for protein expression revealed the apparent decrease of IκBα and up regulatioin of p-p65, p-IκBα and TLR4 in OIR group compared with control. *, P<0.05 comparing between OIR and control group.

Table 2. Vessel-free area, angiogenesis area, vessel number and MG cell count

	OIR group	OIR+ω-3 PUFAs group
Vessel-free area ratio (%)	15.19±1.24	9.26±0.81*
De novo angiogenesis area (%)	1.88±0.13	1.13±0.06*
Vessel number	163.7±2.8	108.6±2.2*
Retinal MG cell count (per 5 mm)	86.3±5.1	52.7±3.4*

Note: *, P<0.05 comparing between OIR and OIR+ω-3 PUFAs group.

MG activation, enhanced TLR4 and NF-κB activity in OIR mouse retinal tissues

Data on cell count of retinal MG cells exhibited significantly more Iba1-positive MG cells within 5 mm length in OIR model mice compared to that in control group (P<0.05) (**Figure 2A**). Flow cytometry results also indicated that, compared to normal control mice, Iba1-positive MG cells in OIR group was remarkably increased (**Figure 2B**). qRT-PCR results showed that, compared to control group, significantly growing levels of TLR4, TNF-α, IL-1β mRNAs were presented in OIR model mice compared to that of normal control (**Figure 2C**). Western blot results further demonstrated that the expressions of TLR4, p-IκBα, and p-p65 protein expression were significantly higher in OIR mice retina than those in normal control (**Figure 2D**).

ω-3 PUFAs inhibited angiogenesis and MG activation, decreased TLR4 expression or NF-κB activity

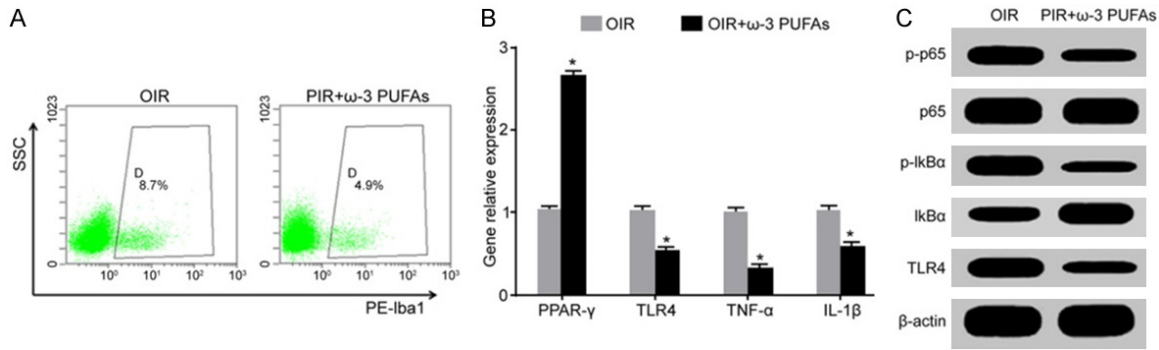Compared to OIR model mice without ω-3 PUFAs injection, the ω-3 PUFAs treatment

Figure 3. ω-3 PUFAs inhibited angiogenesis and MG activation, decreased TLR4 expression or NF-κB activity. A. Flow cytometry detected the Iba1 positive rate in retina and illustrated that the rate was down regulated by the treatment of ω-3 PUFAs; B. qRT-PCR for mRNA expression unraveled that ω-3 PUFAs led to the reduction of TLR4, p-IκBα, p-p65 protein expression and increase of PPAR-γ level; C. Western blot for protein expression showed that the ω-3 PUFAs reversed the effect of OIR and resulted in the increase of IκBα and reduction of p-p65, p-IκBα and TLR4. *, P<0.05 comparing between OIR and OIR+ω-3 PUFAs group.
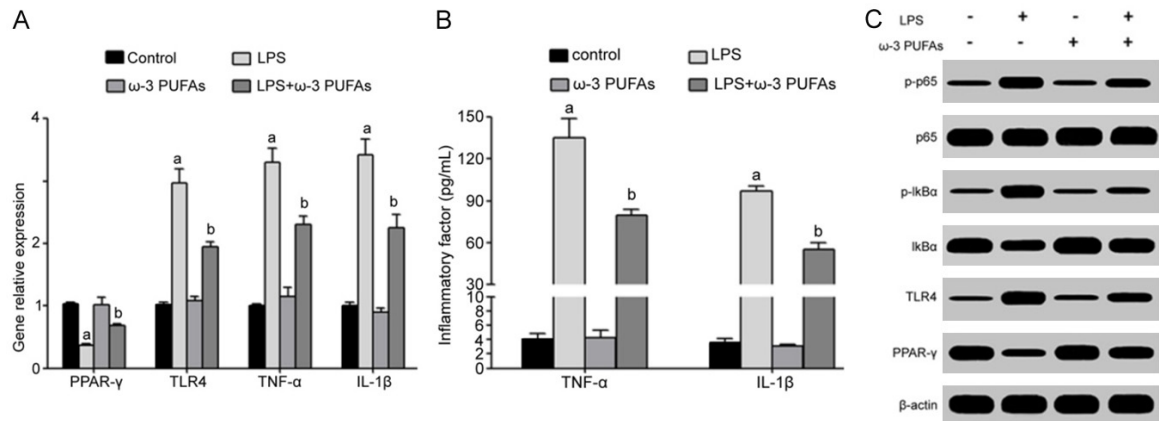

Figure 4. ω-3 PUFAs suppressed LPS-induced activation of MG via up-regulating PPAR-γ. A. qRT-PCR for mRNA expression demonstrated that LPS led to the reduction of PPAR-γ and up regulation of TLR4, p-IκBα, p-p65, while ω-3 PUFAs to some extent counteracted the regulatory role of LPS; B. ELISA was applied to measure the inflammatory factor contents in MG culture supernatants and illuminated that TNF-α, IL-1β levels were induced by LPS, but ω-3 PUFAs limited the promoting effect of LPS on TNF-α, IL-1β; C. Western blot for protein expression showed the obvious decrease of IκBα and rise of p-p65, p-IκBα and TLR4 in LPS group compared with control. However, the expression of IκBα was elevated and levels of p-p65, p-IκBα and TLR4 were depleted in LPS+ω-3 PUFAs group compared with LPS group. a, P<0.05 comparing between LPS group and control group; b, P<0.05 comparing between LPS+ω-3 PUFAs and LPS group.

induced significant drop of vessel-free area ratio, angiogenesis area ratio and vessel number in OIR mice (**Table 2**), indicating that ω-3 PUFAs could inhibit retinal angiogenesis. Count of retinal MG cells showed that ω-3 PUFAs injection remarkably lowered the number of Iba1 positive MG cells in 5 mm length compared to OIR model mice (**Table 2**). Flow cytometry results validated that Iba1 positive MG cell ratio in retinal tissues of OIR model mice treated with ω-3 PUFAs was notably diminished compared to OIR model mice (**Figure 3A**). Moreover, qRT-PCR results unveiled that, compared to OIR model mice without the treatment,

ω-3 PUFAs significantly reduced TLR4, TNF-α and IL-1β mRNA expression, whilst PPAR-γ mRNA expression was significantly elevated (P<0.05) (**Figure 3B**). In western blot detection, we found that, compared to OIR model mice, the injection of ω-3 PUFAs in OIR model mice caused significantly lower TLR4, p-IκBα or p-p65 protein expression and rising level of PPAR-γ protein (**Figure 3C**).

ω-3 PUFAs suppressed LPS-induced activation of MG via up-regulating PPAR-γ

As MG participates in retinal angiogenesis during RNDs such as oxygen-induced retinopathy
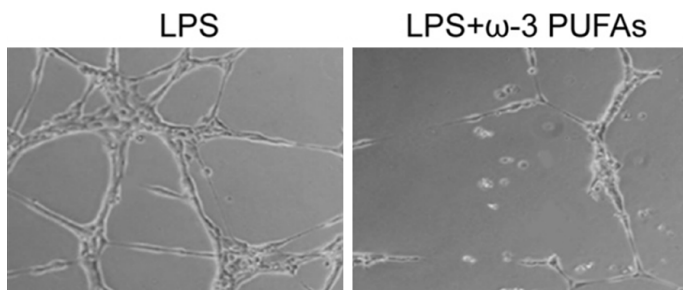
Figure 5. Tube formation assay. ω-3 PUFAs inhibited the formation of tube.

(OIR) and DR, our *in vitro* test further investigate whether ω-3 PUFAs affects the activation of MG. qRT-PCR results showed that, compared to control group, the treatment of LPS remarkably decreased PPAR-γ mRNA expression, while induced the growing levels of TLR4, TNF-α and IL-1β mRNA expression, which were consistent with the changes in OIR model mice. Interestingly, ω-3 PUFAs treatment had no significant effects on PPAR-γ, TLR4, TNF-α or IL-1β mRNA expression level, but alleviated the impact of LPS on the expressions of PPAR-γ, TLR4, TNF-α and IL-1β (**Figure 4A**). ELISA results confirmed that ω-3 PUFAs significantly weakened LPS-induced synthesis and release of MG inflammatory factors TNF-α and IL-1β (**Figure 4B**). Western blot results implicated that, LPS treatment significantly down-regulated PPAR-γ protein expression in MG cells, and facilitated TLR4/NF-κB signal pathway (**Figure 4C**).

ω-3 PUFAs inhibited tube formation in HUVEC-MG co-culture system

Of note, tube formation assay was employed to evaluate the proliferation of cells. The result showed that, compared to LPS treatment, ω-3 PUFAs intervention further extremely decreased tube formation number in the co-culture system (**Figure 5**).

Discussion

RND is mainly treated by retinal laser coagulation, or extra-sclera frozen, both of which are traumatic surgery and may bring severe complications such as night blindness, peripheral vision deficit and lower visual sensitivity. Recently, the application of anti-VEGF drugs has obtained certain progress but still has infectious risks plus higher cost [2]. Meanwhile,

inhibition of VEGF may also disrupt normal retinal vascular development or cause retinal neuron dysfunction [3]. Therefore, the investigation of RND pathogenesis and identification of novel treatment targets is still the major research focus in ophthalmology nowadays.

Retina is consisted of regularly arranged neurons and peripheral glia cells. Microglia (MG) has the smallest volume and occupies about 10%~20% of all retina glial cells [15, 16]. MG locates in CNS and retinal tissues. As similar with those MG from CNS, retinal MG cells also derive from myeloid progenitor cells in monocyte-macrophage lineage. Retinal MG has immune modulation effects, and is involved in multiple processes including neurodevelopment, angiogenesis and traumatic repair [9, 17, 18]. Retinal MG is the only known innate antigen presenting cells (APCs) in retina, and can recognize pathogenic microbes or endogenous ligand via cell surface modular recognition receptor to up-regulate MHC-II type antigen presenting and co-stimulating molecules (CD86, CD80 and CD40), to secret inflammatory factors TNF-α and IL-1β, thus is important for inducing immune response, anti-infection, non-infectious inflammation and pathological angiogenesis [16, 19]. Toll-like receptors (TLRs) belong to a group of innate immune modular recognition receptor. TLR4 has been widely studied as it can be activated by endogenous ligands to induce inflammatory response. Recent study showed that TLR4-induced inflammatory response facilitated retinal angiogenesis [20]. Moreover, lipopolysaccharide (LPS) treatment can aggravate pathology of OIR model rats, and result in retinal angiogenesis. As LPS is the effective agonist of TLR4, it has been applied as a critical modular recognition receptor on retinal MG surface. Therefore we speculated that LPS participated in pathological angiogenesis in retinal tissues via regulating TLR4 and the activities of MG cells.

ω-3 PUFAs belongs to long chain poly-unsaturated fatty acids, and mainly consists of eicosapetaenoic acid (EPA) and doeosahexaeoic acid (DHA). It can provide energy sources and substrate for the body. In addition to nutrition values, multiple studies found that ω-3 PUFAs exerted anti-inflammation and immune modu-

lation effects via multiple mechanisms [21, 22]. ω-3 PUFAs can replace arachidonic acid (AA) in cell membrane phospholipid, and suppress AA oxidation by cyclooxygenase and lipid peroxidase. It significantly inhibit phospholipase A2 activity, decrease AA-derived inflammatory metabolites leukotriene 4 (LTB4) and thromboxane A2 (TXA2) release for alleviating inflammatory response [21, 22]. ω-3 PUFAs can also modulate immune functions via adjusting adhesion molecule expression, enhancing synthesis of anti-inflammatory transmitter, inhibiting platelet activating factor, and decreasing microvessel permeability [6, 23]. Recent study showed that ω-3 PUFAs also suppressed TLR4-induced NF-κB signal pathway activation, target gene expression and inflammatory factor release, all of which form novel mechanism under anti-inflammation of ω-3 PUFAs [24]. Therefore, we proposed that ω-3 PUFAs might suppress TLR4/NF-κB signal pathway activation in retinal MG cells via activating its receptor PPAR-γ expression, further suppressing synthesis, expression and release of inflammatory factors in MG cells, thus inhibiting retinal angiogenesis.

OIR model has been widely used for studying retinal angiogenesis, and is one of animal models in studying RNDs such as ROP and DR. Therefore, this study generated a mouse OIR model, on which ω-3 PUFAs was injected via tail veins to observe its effects on PPAR-γ, TLR4/NF-κB signal pathway or inflammatory factors TNF-α and IL-1β in MG cells, and its effects on mouse retinal angiogenesis. Kataoka et al showed significantly increased Iba1 positive MG cells in OIR model mice [25], and abundant distribution around newly formed vessels, indicating the role of MG activation in facilitating OIR mouse retinal angiogenesis. Rungger et al found direct correlation between enhanced MG cell number or activation and retinal angiogenesis in DR rats [10]. Eter et al performed *in vivo* imaging on an animal model having choroidal angiogenesis induced by retinal laser coagulation, and showed recruitment of CX3CR1-positive MG cells at 60min after laser injury, and persistence of MG until day 35 [26]. In this study, OIR model mice showed elevated retinal angiogenesis, accompanied with enhanced number and activation of MG, as consistent with Kataoka et al [25], Rungger et al [10] and Eter et al [26]. Moreover, Kataoka et al showed that after removing retinal MG cells by clodro-

nate liposomes, retinal angiogenesis in OIR model mice was inhibited by 59.0% [25], proving the role of MG cells in retinal angiogenesis. After *in vivo* injection of ω-3 PUFAs, OIR model mice showed significantly elevated PPAR-γ expression in retinal tissues, plus decreased expression of TLR4, NF-κB activity and inflammatory factor levels, and inhibition of retinal angiogenesis or MG cell activation. Connor et al showed that orally intake of ω-3 PUFAs significantly inhibited retinal angiogenesis and alleviated OIR [4], as similar with our results. Kim et al showed that ω-3 PUFAs significantly inhibited TLR4 recruitment, impeded NF-κB signal transduction, and alleviated ischemia-reperfusion induced hepatocyte injury [27], partially sharing similar results with our study showing the blockade of TLR4/NF-κB signal transduction activity by ω-3 PUFAs. Stahl et al found that the inhibitory role of ω-3 PUFAs on retinal angiogenesis depends on PPAR-γ activation, and was correlated with decreased expression of inflammatory factor TNF-α, adhesion molecule ICAM-1 and VCAM-1 [5]. The inhibition of PPAR-γ weakened the inhibitory role of ω-3 PUFAs on retinal angiogenesis. Wang et al showed that enhancement of PPAR-γ activation significantly decreased TLR4 expression, weakened activation of U937 cells by LPS and release of inflammatory factor TNF-α [12]. Li et al found that LPS stimulus enhanced NF-κB signal pathway activity and induced inflammatory response in renal cell line HK-2, whilst ω-3 PUFAs treatment significantly up-regulated PPAR-γ expression, and weakened activation of NF-κB signal pathway by LPS [8]. Currently, our data unveiled the regulation of PPAR-γ/TLR4/NF-κB signal pathway by ω-3 PUFAs in the development of retinal angiogenesis, which has not been previously reported.

Conclusion

Our data demonstrates that ω-3 PUFAs can inhibit retinal MG cell activation and retinal angiogenesis via up-regulating PPAR-γ expression, down-regulating TLR4 expression and inactivating NF-κB signal pathway to reduce inflammatory factor release, which provides peer insights for the future therapy of retinal angiogenesis.

Acknowledgements

Disclosure of conflict of interest

None.

Address correspondence to: Drs. Yanfang Zhang and Xueyan Wang, Department of Ophthalmology, Xiangyang Central Hospital, Affiliated Hospital of Hubei University of Arts and Science, 39 Jingzhou Street, Xiangcheng Distrct, Xiangyang, Hubei, China. Tel: +86-713-3324530; Fax: +86-713-3324530; E-mail: yanfangzhangg@163.com (YFZ); xueyanwangf@163.com (XYW)

References

[1] Bradley J, Ju M and Robinson GS. Combination therapy for the treatment of ocular neovascularization. Angiogenesis 2007; 10: 141-8.

[2] Nicholson BP and Schachat AP. A review of clinical trials of anti-VEGF agents for diabetic retinopathy. Graefes Arch Clin Exp Ophthalmol 2010; 248: 915-30.

[3] Saint-Geniez M, Maharaj AS, Walshe TE, Tucker BA, Sekiyama E, Kurihara T, Darland DC, Young MJ and D'Amore PA. Endogenous VEGF is required for visual function: evidence for a survival role on muller cells and photoreceptors. PLoS One 2008; 3: e3554.

[4] Connor KM, SanGiovanni JP, Lofqvist C, Aderman CM, Chen J, Higuchi A, Hong S, Pravda EA, Majchrzak S, Carper D, Hellstrom A, Kang JX, Chew EY, Salem N Jr, Serhan CN and Smith LE. Increased dietary intake of omega-3-polyunsaturated fatty acids reduces pathological retinal angiogenesis. Nat Med 2007; 13: 868-73.

[5] Stahl A, Sapieha P, Connor KM, Sangiovanni JP, Chen J, Aderman CM, Willett KL, Krah NM, Dennison RJ, Seaward MR, Guerin KI, Hua J and Smith LE. Short communication: PPAR gamma mediates a direct antiangiogenic effect of omega 3-PUFAs in proliferative retinopathy. Circ Res 2010; 107: 495-500.

[6] Wall R, Ross RP, Fitzgerald GF and Stanton C. Fatty acids from fish: the anti-inflammatory potential of long-chain omega-3 fatty acids. Nutr Rev 2010; 68: 280-9.

[7] Kaplins'kyĭ SP, Shysh AM, Nahibin VS, Dosenko VIe, Klimashevs'kyĭ VM, Moĭbenko OO. Omega-3 polyunsaturated fatty acids stimulate the expression of PPAR target genes. Fiziol Zh 2009; 55: 37-43.

[8] Li H, Ruan XZ, Powis SH, Fernando R, Mon WY, Wheeler DC, Moorhead JF and Varghese Z. EPA and DHA reduce LPS-induced inflammation responses in HK-2 cells: evidence for a PPAR-gamma-dependent mechanism. Kidney Int 2005; 67: 867-74.

[9] Rigato C, Buckinx R, Le-Corronc H, Rigo JM and Legendre P. Pattern of invasion of the embryonic mouse spinal cord by microglial cells at the time of the onset of functional neuronal networks. Glia 2011; 59: 675-95.

[10] Rungger-Brandle E, Dosso AA and Leuenberger PM. Glial reactivity, an early feature of diabetic retinopathy. Invest Ophthalmol Vis Sci 2000; 41: 1971-80.

[11] Zeng XX, Ng YK and Ling EA. Neuronal and microglial response in the retina of streptozotocin-induced diabetic rats. Vis Neurosci 2000; 17: 463-71.

[12] Wang CZ, Zhang Y, Li XD, Hu Y, Fang ZG, Lin DJ, Xiao RZ, Huang RW, Huang HQ, Liu PQ and Liu JJ. PPARgamma agonist suppresses TLR4 expression and TNF-alpha production in LPS stimulated monocyte leukemia cells. Cell Biochem Biophys 2011; 60: 167-72.

[13] Zhang LL, Gao CY, Fang CQ, Wang YJ, Gao D, Yao GE, Xiang J, Wang JZ and Li JC. PPARgamma attenuates intimal hyperplasia by inhibiting TLR4-mediated inflammation in vascular smooth muscle cells. Cardiovasc Res 2011; 92: 484-93.

[14] Li Z, He T, Du K, Xing YQ, Run YM, Yan Y and Shen Y. Inhibition of oxygen-induced ischemic retinal neovascularization with adenoviral 15-lipoxygenase-1 gene transfer via up-regulation of PPAR-gamma and down-regulation of VEGFR-2 expression. PLoS One 2014; 9: e85824.

[15] Koso H, Tsuhako A, Lai CY, Baba Y, Otsu M, Ueno K, Nagasaki M, Suzuki Y and Watanabe S. Conditional rod photoreceptor ablation reveals Sall1 as a microglial marker and regulator of microglial morphology in the retina. Glia 2016; 64: 2005-24.

[16] Ulbrich F, Goebel U, Bohringer D, Charalambous P, Lagreze WA and Biermann J. Carbon monoxide treatment reduces microglial activation in the ischemic rat retina. Graefes Arch Clin Exp Ophthalmol 2016; 254: 1967-1976.

[17] Paques M, Simonutti M, Augustin S, Goupille O, El Mathari B and Sahel JA. In vivo observation of the locomotion of microglial cells in the retina. Glia 2010; 58: 1663-8.

[18] Albini TA, Wang RC, Reiser B, Zamir E, Wu GS and Rao NA. Microglial stability and repopulation in the retina. Br J Ophthalmol 2005; 89: 901-3.

[19] Penfold PL, Wong JG, Gyory J and Billson FA. Effects of triamcinolone acetonide on microglial morphology and quantitative expression of MHC-II in exudative age-related macular degeneration. Clin Exp Ophthalmol 2001; 29: 188-92.

[20] He C, Sun Y, Ren X, Lin Q, Hu X, Huang X, Su SB, Liu Y and Liu X. Angiogenesis mediated by toll-like receptor 4 in ischemic neural tissue. Arterioscler Thromb Vasc Biol 2013; 33: 330-8.

[21] Singer P, Shapiro H, Theilla M, Anbar R, Singer J and Cohen J. Anti-inflammatory properties of omega-3 fatty acids in critical illness: novel mechanisms and an integrative perspective. Intensive Care Med 2008; 34: 1580-92.

[22] Machado Andrade Pde M and Tavares do Carmo M. Dietary long-chain omega-3 fatty acids and anti-inflammatory action: potential application in the field of physical exercise. Nutrition 2004; 20: 243.

[23] Liu T and Li G. Anti-inflammatory effects of long-chain omega 3 fatty acids: potential benefits for atrial fibrillation. Med Hypotheses 2005; 65: 200-1.

[24] Yi C, Bai X, Chen J, Chen J, Li J, Liu P and Liao Y. Effect of omega-3 polyunsaturated fatty acid on toll-like receptors in patients with severe multiple trauma. J Huazhong Univ Sci Technolog Med Sci 2011; 31: 504-8.

[25] Kataoka K, Nishiguchi KM, Kaneko H, van Rooijen N, Kachi S and Terasaki H. The roles of vitreal macrophages and circulating leukocytes in retinal neovascularization. Invest Ophthalmol Vis Sci 2011; 52: 1431-8.

[26] Eter N, Engel DR, Meyer L, Helb HM, Roth F, Maurer J, Holz FG and Kurts C. In vivo visualization of dendritic cells, macrophages, and microglial cells responding to laser-induced damage in the fundus of the eye. Invest Ophthalmol Vis Sci 2008; 49: 3649-58.

[27] Kim K, Jung N, Lee K, Choi J, Kim S, Jun J, Kim E and Kim D. Dietary omega-3 polyunsaturated fatty acids attenuate hepatic ischemia/reperfusion injury in rats by modulating toll-like receptor recruitment into lipid rafts. Clin Nutr 2013; 32: 855-62.